Wind and Structures, Vol. 7, No. 1 (2004) 41-54
DOI: http://dx.doi.org/10.12989/was.2004.7.1.041

Effects of the yaw angle on the aerodynamic behaviour of the Messina multi-box girder deck section

G. Diana†, F. Resta‡, A. Zasso‡, M. Belloli‡† and D. Rocchi‡†

Mechanical Department, Politecnico di Milano, Via La Masa 34 Milano, Italy

(Received August 4, 2003, Accepted January 8, 2004)

Abstract. An analysis refinement of the Messina Strait suspension bridge project has been recently required, concerning mainly the yaw angle effects on the multi-box deck section aerodynamics and the vortex shedding at low reduced velocities V^*. In particular the possible interaction of the axial flow with the large cross beams has been investigated. An original test rig has been designed at this purpose allowing for both forced motion and free motion aero elastic tests, varying the average angle of attack α and the deck yaw angle β. The hydraulic driven test rig allowed for both dynamic and stationary tests so that both the stationary coefficients and the flutter derivatives have been evaluated for each yaw angle. Specific free motion tests, taking advantage from the aeroelastic features of the section model, allowed also the study of the vortex shedding induced phenomena.

Keywords: wind tunnel; bridge aeroelasticity; yaw angle; flutter derivatives; vortex induced vibrations.

1. Introduction

The Messina suspension bridge project required recently a deeper investigation on aspects concerning wind effects on the original multi-box deck section. To this purpose, a new original test rig has been designed, taking advantage of the very large test section, 14×4 m, of the new wind tunnel at Politecnico di Milano and its facilities.

The renewed interest in the Messina Strait crossing project led to a deeper insight on the aerodynamic behavior of the long span bridge, paying particular attention to the effects induced by the incoming wind direction, in the horizontal plane. Expressing the wind yaw angle β with reference to the bridge longitudinal axis, the static aerodynamic coefficient, as well as the flutter derivatives have always been investigated at a yaw angle of 90 deg. The interest on this topic arise from the geometric shape of the multi-box Messina girder that shows every 30 m, along the longitudinal direction, a transversal beam, connecting the three separated decks together. These transversal beams, having the function of structural connection with the hangers, are characterized by relevant dimensions as can be appreciated in Fig. 1.

Differently from a continuous single box section, showing a more emphasized bi-dimensionality, the presence of, the previously described, discontinuous transversal elements, typical of the multi-

† Full Professor
‡ Assistant Professor
‡† Researcher

Fig. 1 Lower sight of the section model

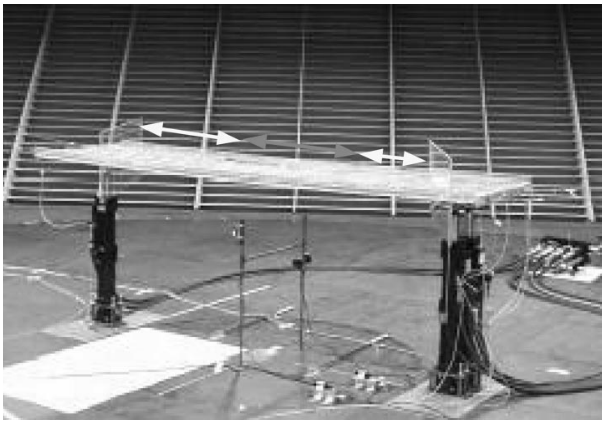

Fig. 2 Whole test rig installed on the turntable

box solution, could generate unexpected phenomena. The beam frontal surface, exposed to the wind, increases together with the wind longitudinal component in the bridge reference system, and, furthermore, the bridge cross section shape, facing the incoming wind, differs from a yaw angle to another. In fact, as a function of the incoming wind direction, the bridge cross section shape, seen by the wind, modifies its geometrical profile, not merely stretching out in the wind direction, but also introducing sharp edges and the contribution of the transversal beams large surfaces. The effects of the wind yaw angle, already faced for traditional single box deck bridges (Zhu, *et al*. 2002, Tanaka, *et al*. 1995), with particular attention to the bride erection stages (Kimura, *et al*. 1994, Scanlan 1993), represent for a multi-box deck sections a relevant topic because of the overmentioned geometric consideration.

In the design stage of the model and experimental rig, a specific interest was to have the possibility to change quickly the yaw angle, to reach this goal the whole experimental rig is installed on the 13 m diameter wind tunnel pneumatic turntable, as visible in Fig. 2. The table allows to change the section yaw angle with no others hardware operations on the experimental rig and model than changing the lateral side screens. Moreover the rig, the model and the experimental set-up has been projected in order to have the possibility to execute both forced and free motion tests, that means to be able to investigate all the relevant aerodynamic aspects in bridge engineering, i.e., static aerodynamic coefficients, flutter derivatives, aerodynamic admittance function and vortex shedding response (Belloli, *et al*. 2003, Zasso 1996). The influence of the yaw angle on all the over mentioned topics has been analyzed.

Considering the available wind speed range, from 1 up to 14 m/s, and the forced motion frequency range, the aerodynamic behavior can be investigated at reduced velocity, V^*, from 1 to 30, including highly non stationary field, $V^*<5$, and quasi-steady conditions, $V^*>10$; the model has been tested with $\beta=90^{\circ}$, $\beta=80^{\circ}$, $\beta=60^{\circ}$ and $\beta=45^{\circ}$.

2. Model, rig and experimental set-up

The 1:60 scale model, 3.6 m long and 1 m wide, the rig and the experimental set-up have been designed to carry out all the cited experimental activities changing the yaw angle.

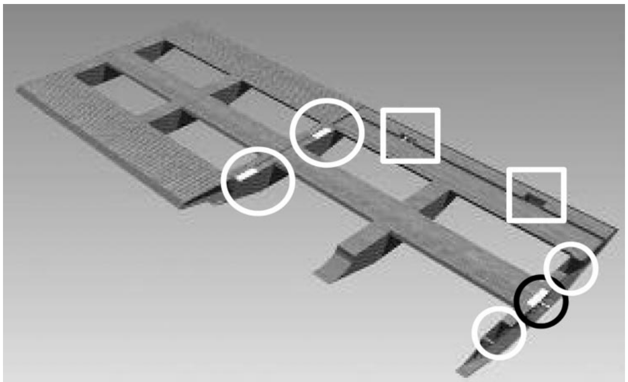

Fig. 3 Bridge deck model structure and transducers locations

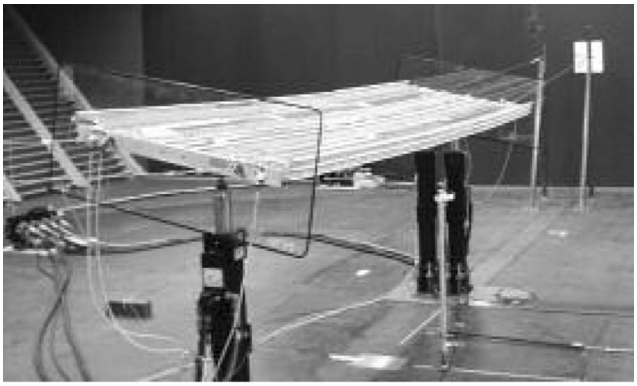

Fig. 4 Model installed in wind tunnel: forced motion test rig

The model is made up by three independent elements, where the central floating one is dynamometric, the two lateral ones are coupled by axial beams (Fig. 3). The dynamometric one, 1 m wide and 1 m long, is constrained to the others by means of springs and preloaded dynamometers, whose positions are highlighted in Fig. 3, able to measure both static and dynamic component of the forces acting on the model, i.e., gravity force, inertia force and aerodynamic force (Belloli, *et al*. 2003).

The two model parts at the sides of the central floating section and two side screens guarantee the correct boundary conditions of the flow field (Figs. 2 and 4), necessary to grant a regular bidimensional flow on the sensible section also for yaw angle up to 45^o. The side screens are oriented according to the wind flow direction for each tested yaw angle, in the 90 deg configuration are 1.25 m wide and 0.5 m high.

The used instrumentation is made up by 7 strain gauge load cells, installed on model, with a maximum load capability of 111 N; key features of these instruments are very high stiffness and high sensibility, suitable to measure aerodynamic forces acting on bridge deck.

Three accelerometers measure bridge deck accelerations, both in vertical and horizontal direction, providing signals for the estimation of inertia force and torque.

Two laser displacement transducers complete the instrumentation, making possible to monitor bridge deck motion by evaluating, with the suitable calibration procedure, the time history of the angle of attack. LVDT installed on hydraulic actuators have been sampled to control forced motion conditions. Two pitot tubes and 2 hot wire anemometer are used to measure wind mean velocity and turbulence index.

Three computer controlled hydraulic actuators, Fig. 4, linked to external cross beam of model, induce forced motion conditions, generating a multi degree of freedom harmonic motion around a user defined average position.

The forced motion configuration is used to execute test to identify the static aerodynamic coefficients and the full set of flutter derivatives.

As far as concern the stationary aerodynamic coefficients, the test procedure provides for the imposition of torsional motion with very low frequency varying angle of attack. To define the full set of flutter derivatives the tests are performed at different imposed frequencies and different wind velocities leading to a wide range of reduced velocity accounting for non stationary conditions and quasi steady conditions.

By means of the same test rig, using the actuators only as rigid links, it is possible to execute aeroelastic tests to check the model response both to turbulent wind and to vortex shedding excitation. This second topic is particularly interesting because of the lack of proven methodology to define the deck behaviour under vortex shedding conditions.

The whole set of test session has been performed with a turbulence level less than 2%.

3. Experimental results

The reference model deck shape, used in the experimental activities, is sketched in Fig. 5, it is a multi-box girder with two lateral road boxes and a central rail one.

This bridge deck configuration represents the results of a parametric optimization on the aerodynamic devices with a couple of trip wires on the lower part of the lateral road boxes. The

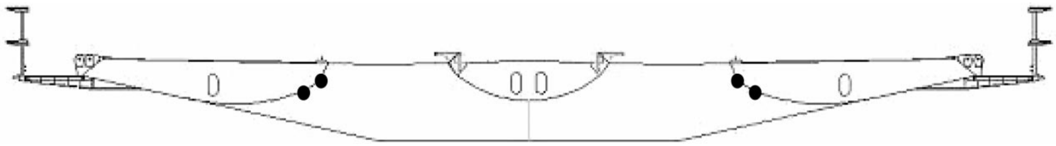

Fig. 5 Adopted reference model to evaluate the yaw angle influence on bridge aerodynamic behaviour

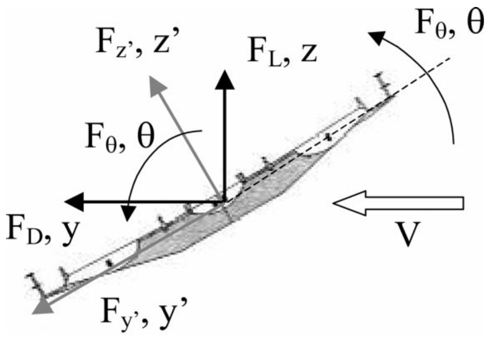

Fig. 6 Adopted reference system

presence of this aerodynamic device deeply affects the deck aerodynamics giving as a result a monotone trend to the moment curve that, in the optimized position of the couple of trip wires, shows very small values and a positive derivative along the whole angle of attack range.

3.1. Influence of the yaw angle on the static coefficients

During the static coefficient procedure, the model is driven to rotate around the bridge longitudinal axis with a very low frequency (0.025 Hz), covering ±10 deg angle of attack.

The correct estimate of the wind forces and, consequently, of the aerodynamic coefficients, needs an accurate depuration of the gravity effects and inertia effects. The adopted procedure consists in a

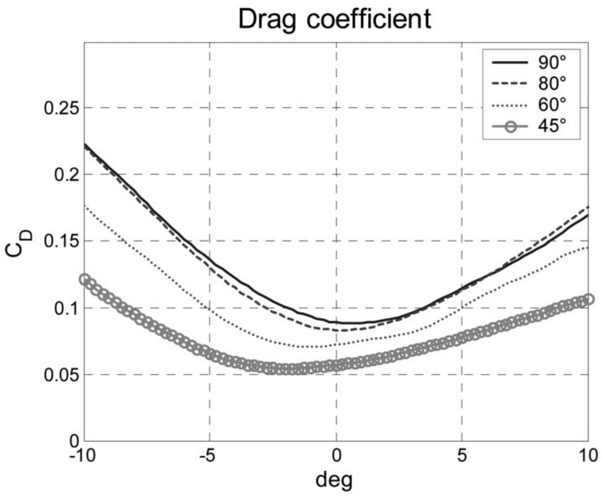

Fig. 7 C_D for the twin trip wire configuration at different yaw angles

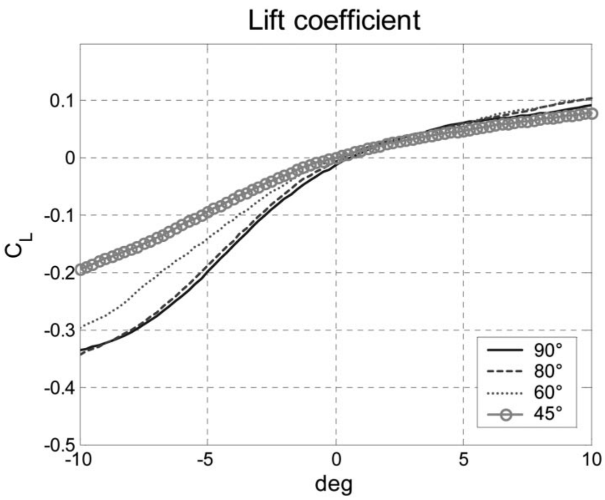

Fig. 8 C_L for the twin trip wire configuration at different yaw angles

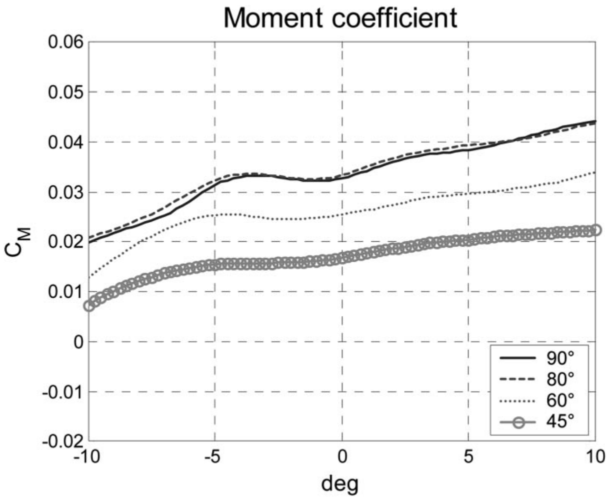

Fig. 9 C_M for the twin trip wire configuration at different yaw angles

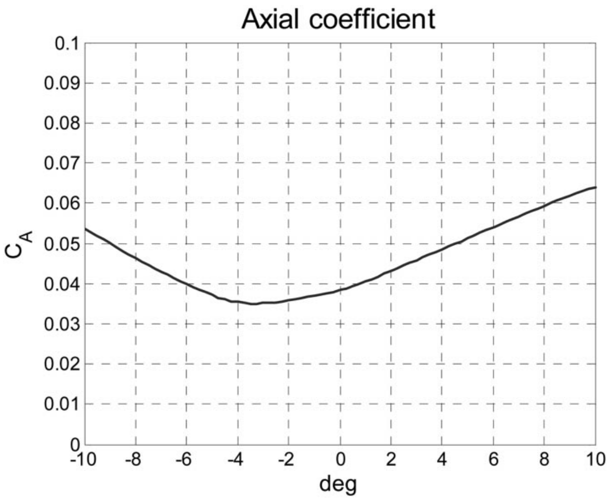

Fig. 10 C_A for the twin trip wire configuration at different yaw angles at 45 deg yaw angle

double test during which exactly the same harmonic oscillation is given to the model with and without the blowing wind. The aerodynamic force can be evaluated by subtracting the forces measured in still air and in wind condition. The complete procedure and data analysis methodology is described in Belloli, *et al*. (2003).

All the coefficients will be expressed in the bridge global reference system, following the convention shown in Fig. 6. This reference system is assumed rotating together with the model around the vertical axis, when the wind-bridge yaw angle is considered.

From Fig. 7 to Fig. 10 the static coefficients for the twin trip wire configuration are plotted for different yaw angles including also the usual β=90 deg (wind perpendicular to the bridge).

The coefficients are normalised adopting the forces expressed in the bridge reference system and the mean wind velocity measured in the global wind tunnel reference system.

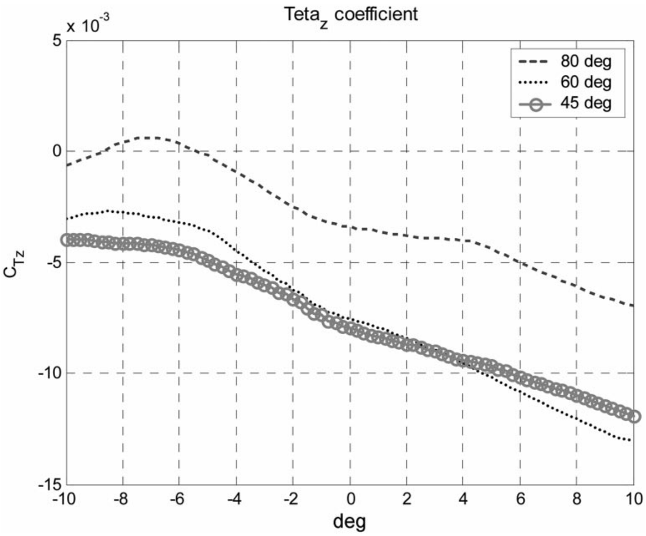

Fig. 11 Yaw moment coefficient C_{tz} for the twin trip wire configuration at different yaw angles

The drag coefficient (Fig. 7) decreases together with the yaw angle, also due to the reduction of the cross-bridge wind component. Furthermore the minimum in the coefficient trend moves towards negative angle of attack decreasing the yaw angle. Concerning the lift coefficient (Fig. 8), similar considerations can be stressed, indicating no lifting effects for the bridge longitudinal wind component, and resulting in an average reduction of the lift derivative.

Similar considerations hold for the moment coefficient: a general reduction of the moment derivative is shown decreasing the yaw angle, justified by the no lifting effects of the axial wind component. On the other hand a general shift of the absolute values appears and, decreasing the yaw angle, the coefficient trend versus the angle of attack seems to be more linear. The axial coefficient shows negligible values for high yaw angles reaching the 40% of the drag coefficient at β=45 deg as shown in Fig. 10.

In Fig. 11 the value of the yaw moment coefficient C_{tz} is reported versus the angle of the attack for different yaw angles (β=80 deg, β=60 deg, β=45 deg).

3.2. Influence of the yaw angle on the flutter derivatives

The flutter derivatives definition follows the formulation presented by Zasso in (1996):

$$F_y = qBL\left(-p_1^*\frac{i\omega z}{V} + p_4^*\frac{\pi}{2V^{*2}}\frac{z}{B} - p_2^*\frac{i\omega B\theta}{V} + p_3^*\theta - p_5^*\frac{i\omega y}{V} + p_6^*\frac{\pi}{2V^{*2}}\frac{y}{B}\right)$$

$$F_z = qBL\left(-h_1^*\frac{i\omega z}{V} + h_4^*\frac{\pi}{2V^{*2}}\frac{z}{B} - h_2^*\frac{i\omega B\theta}{V} + h_3^*\theta - h_5^*\frac{i\omega y}{V} + h_6^*\frac{\pi}{2V^{*2}}\frac{y}{B}\right) \tag{1}$$

$$F_\theta = qB^2L\left(-a_1^*\frac{i\omega z}{V} + a_4^*\frac{\pi}{2V^{*2}}\frac{z}{B} - a_2^*\frac{i\omega B\theta}{V} + a_3^*\theta - a_5^*\frac{i\omega y}{V} + a_6^*\frac{\pi}{2V^{*2}}\frac{y}{B}\right)$$

being q the dynamic pressure, B the deck chord, L the length of the dynamic part of the model and V the upstream wind velocity. This formulation allows to better investigate the flutter derivative coefficient in the low reduced velocity range.

Flutter derivatives coefficients are functions of three quantities, which are: reduced velocity, average angle of attack and yaw angle. Vertical, torsional and horizontal tests are all required to define flutter derivatives and combined motion tests are useful to check the obtained results.

Tests have been performed imposing a mono harmonic motion law to the section model on the vertical or torsional degree of freedom or on both of them. The frequencies f of the sinusoidal forced motion are in the field $0.2 < f < 4$ Hz.

Analyzing the flutter derivatives at different yaw angles β, a similar trend vs. V^* is shown in the following figures. At high V^* all the data show an asymptotic behavior confirming the quasi steady

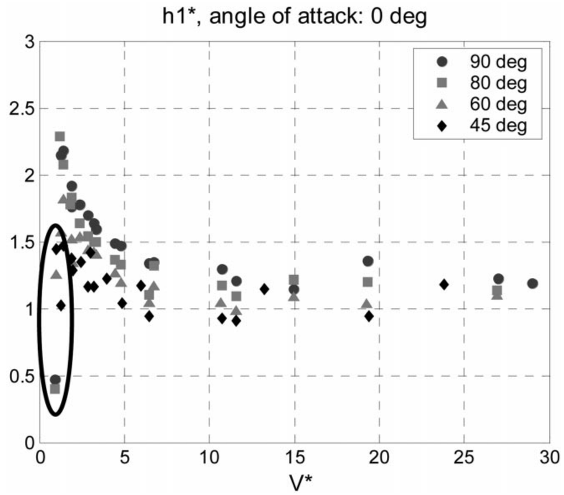

Fig. 12 h_1^* coefficient varying the yaw angle

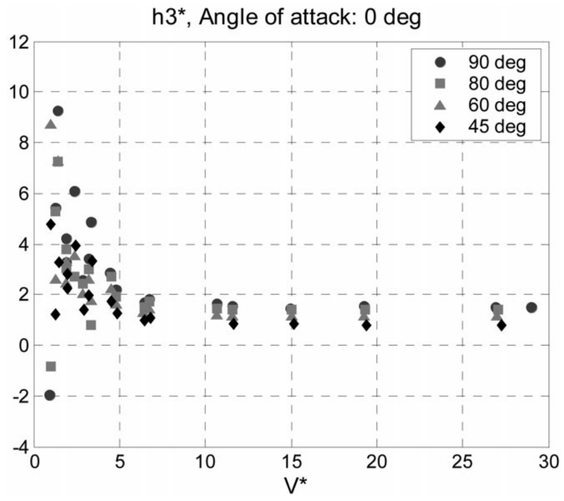

Fig. 13 h_3^* coefficient varying the yaw angle

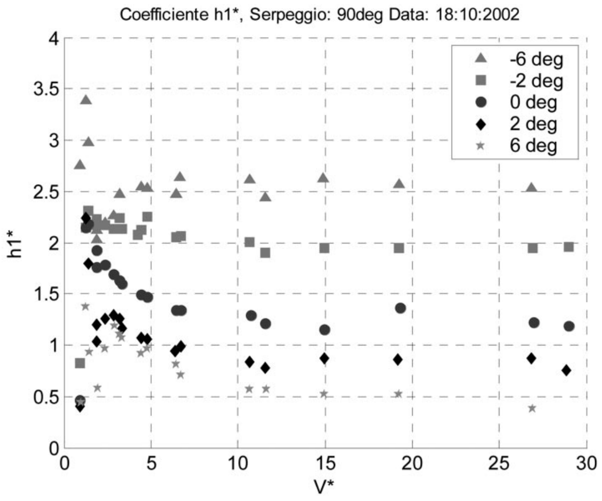

Fig. 14 h_1^* varying the angle of attack at β=90 deg

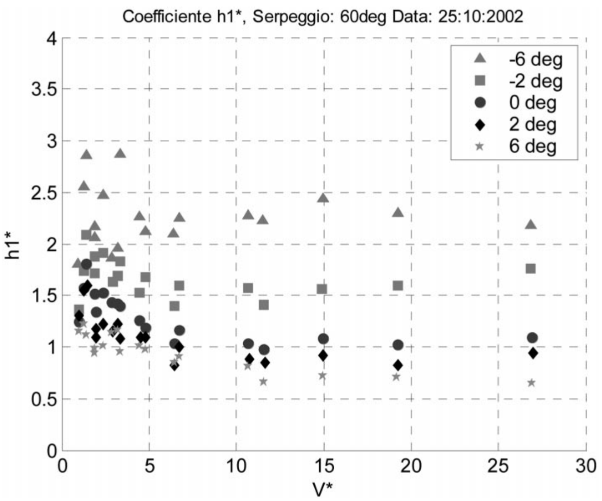

Fig. 15 h_1^* varying the angle of attack at β=60 deg

theory. Fig. 12 confirms, for the h_1^* coefficient at high reduced velocity, a trend coherent with the dependence of the lift derivatives on β at 0 deg angle of attack: as shown in Fig. 12, the lift derivative is clearly higher at β=90 deg decreasing together with the yaw angle.

On the other hand, the low V^* region is always characterized by a high V^* dependence in the coefficients.

Same considerations can be stressed on the h_3^* coefficient as shown in Fig. 13.

Figs. 14 and 16 report h_1^* coefficient varying the angle of attack for two yaw angles respectively β=90 deg and β=60 deg.

A correct asymptotic trend towards the quasi steady theory (Figs. 7 and 8) values can be observed at high reduced velocities.

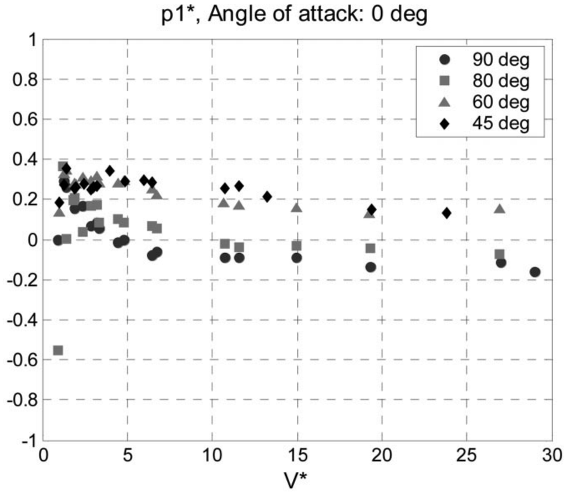

Fig. 16 p_1^* coefficient varying the yaw angle

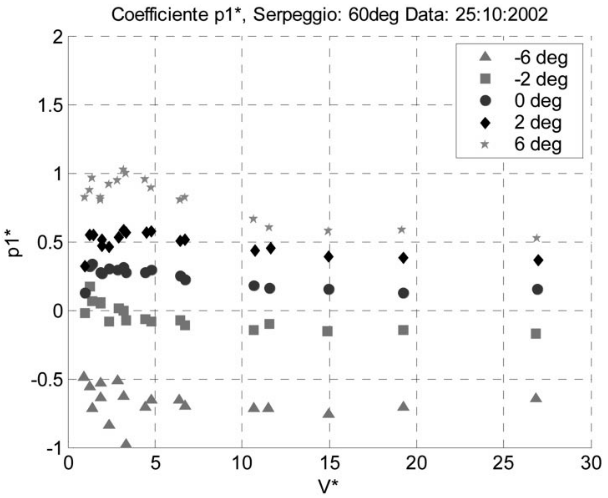

Fig. 17 p_1^* coefficient varying the angle of attack, $\beta = 60$ deg

Finally in Fig. 16 the p_1^* coefficient vs the V^* is reported, at high V^* values according to the quasi steady theory an increase of the coefficient for a reduction of the yaw angle is bound to an increase of the drag derivative at 0 deg angle of attack as shown in Fig. 7.

As an example the p_1^* trend versus the angle of attack is reported for the 60 deg yaw angle configuration in Fig. 17.

3.3. Influence of the yaw angle β on the flutter velocity

The flutter velocity threshold is calculated considering three natural modes, in particular the considered modal shapes are the first vertical, the first torsional and the first horizontal one.

Table 1 Yaw angle influence on the flutter velocity

β [deg]	α [deg]	Flutter velocity [m/s]
90	+2	106
80	+2	116
60	+2	133
45	+2	147

The appropriate set of flutter derivatives is taken into account in defining the aeroelastic forces acting on the bridge deck, that means that at each yaw angle the corresponding flutter derivatives are used (Diana 1995).

The so calculated flutter velocities are reported in Table 1. As visible the most severe conditions are for β=90 deg.

3.4. Influence of the yaw angle β on the vortex shedding

The power input due to vortex shedding has been investigated by means of free motion tests (Belloli 2003). The section model has been rigidly linked to its extremities, free of vibrating according to its first flexural mode at 5.1 Hz. Tests in still air have been also performed, defining the structural non dimensional damping h_{stl}, observing the system response (Fig. 18) to an initial condition representative of the only first flexural mode (h_{stl} = 0.6%). Tests performed at different V^* in the ranges $0.4<V^*<0.6$ and $1.0<V^*<1.2$, showed acceleration time histories like the one plotted in Fig. 19. It is clearly visible the aeroelastic effect due to the wind energy input, reducing at first the global damping of the structure to negative values and reaching finally a balance between aerodynamic energy input and structural dissipation at high amplitudes.

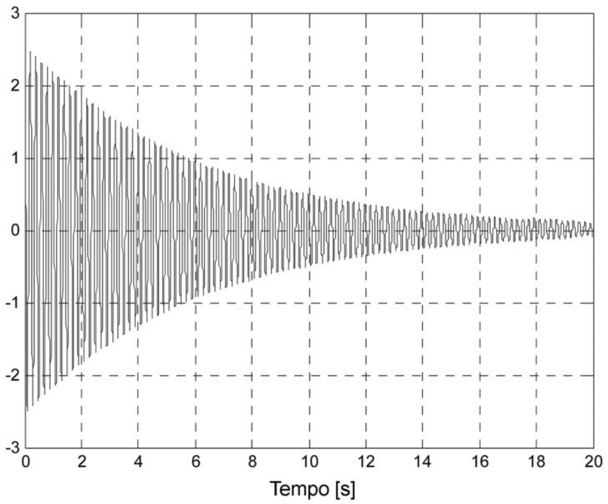

Fig. 18 Flexural mode decay in still air

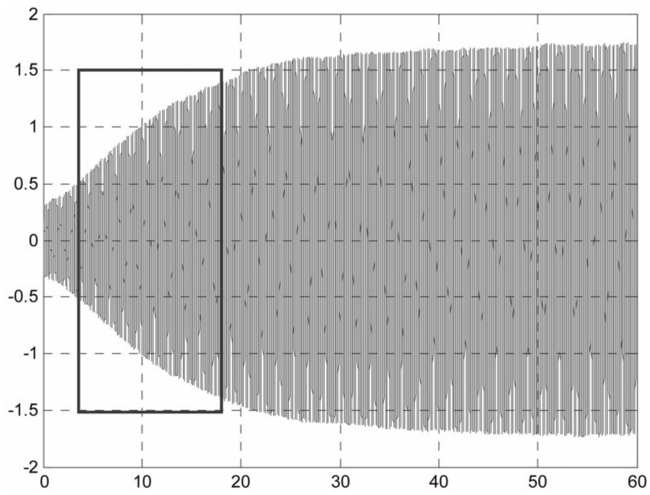

Fig. 19 Vortex shedding excitation build up

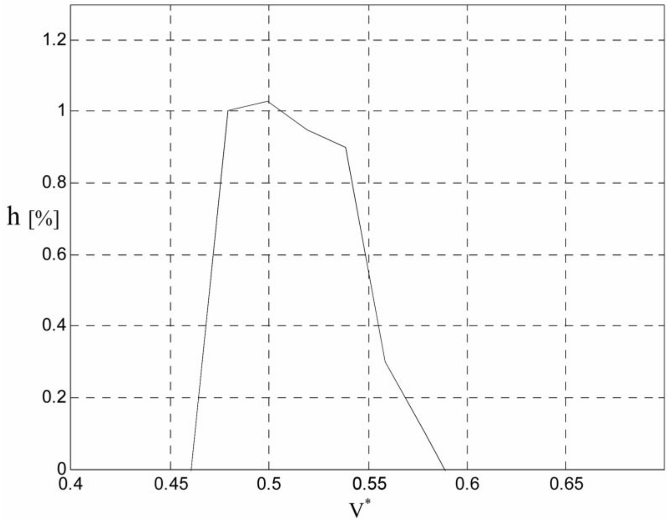

Fig. 20 Vortex shedding lock-in range at yaw angle 90 deg

During the build up stage of the system wind response is possible to evaluate the non dimensional damping h_{wind} in a way similar to the structural one. The phenomenon is bounded to the vortex shedding that, around specific critical V^* is locked to the first flexural natural frequency.

In Fig. 20 the maximum aerodynamic non dimensional damping ($h = -h_{stl} + h_{wind}$) given by the build-up tests has been plotted as a function of V^* at 90 deg yaw angle: the lock-in range is centered around a $V^*=0.5$.

The performed tests showed the presence of another lock-in region at $V^*=1$ as visible in Fig. 21 where the normalized acceleration reached at the model mid-span is reported.

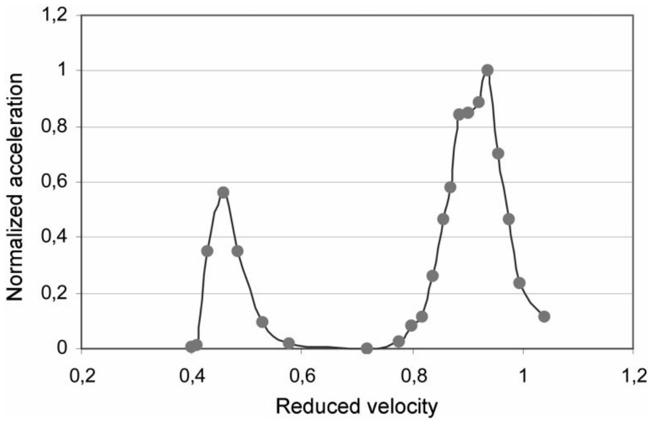

Fig. 21 Vortex shedding lock-in ranges at yaw angle 90 deg

Table 2 Yaw angle influence on vortex shedding

Yaw angle β	90	80	60	45
V^*	0.5	0.45	1.16	1.0
h [%]	1.1	0.78	0.6	<0.6

Repeating the analysis varying the yaw angle, the results summarized in Table 2 have been found, showing the presence of the vortex shedding also at yaw angles different from β=90 deg, but with reduction of severity in terms of energy input and with a synchronism range centered around $V^*=1$ for β=45÷60 deg.

Results are in agreement with the flutter derivatives reported in Fig. 12 showing at $V^*=0.5$ a trend towards negative values. In particular it can be seen that decreasing the yaw angle the h_1^* (Fig. 12) coefficients show higher values denoting a more stable behaviour with respect to the vortex shedding excitation.

4. Conclusions

The influence of the yaw angle on the Messina section aerodynamics was found not critical. In particular, both the stationary and non-stationary coefficients showed the same trend versus the angle of attack, with only a reduction of the absolute values. The effects in terms of axial loads showed forces reaching at β=45 deg values around 40% of the section drag coefficient defined at β=0 deg. The analysis of the data allowed to conclude that the cross beams presence underneath the deck doesn't play any relevant role in the aerodynamic parameters governing the bridge stability. Specific tests have been finally arranged to analyze the vortex shedding excitation of the multi-box deck section as a function of the yaw angle β, resulting again in a reduction of the related effects. In particular two ranges of critical V^* have been encountered, $0.4<V^*<0.6$ and $1.0<V^*<1.2$ and the maximum vortex shedding excitation shifted from the first to the second field decreasing the yaw angle β from 90 to 45 deg.

References

Belloli, M., Bocciolone, M., Resta, F. and Tosi, A. (2003), "Forced motion and free motion aeroelastic tests on a new concept dynamometric section model of the Messina suspension bridge", *Int. Conf. on Wind Engineering*, Lubbock, Texas.

Diana, G., *et al.* (1995), "Comparison between wind tunnel tests on a full aeroelastric model for the proposed bridge over Stretto di Messina and numerical results", *J. Wind Eng. Ind. Aerodyn*, **54/55**, 101-113.

Kimura, K., Nakamura, S. and Tanaka, H. (1994), "Buffeting analysis for cable-stayed bridges during construction in yawed wind", *Proc. Symp. on Cable Stayed and Suspension Bridges*, Deauville, France.

Scanlan, R.H. (1993), "Bridge buffeting by skew winds in erection stages", *J. Eng. Mech.*, **119**(2), 251-261, ASCE.

Tanaka, H., Kimura, K., Nakamura, S. and Larose, G.L. (1995), "Effects of wind yaw angles on bridge response", *Int. Conf. on Wind Engineering*, New Delhi, India.

Zasso, A. (1996), "Flutter derivatives: advantages of a new representation convention", *J. Wind Eng. Ind. Aerodyn.*, **60**, 35-47, Elsevier.

Zhu, L.D., Xu, Y.L. and Xiang, H.F. (2002), "Tsing Ma bridge deck under skew winds - Part I: aerodynamic coefficients", *J. Wind Eng. Ind. Aerodyn*, **90**, 781-805.

Zhu, L.D., Xu, Y.L. and Xiang, H.F. (2002), "Tsing Ma bridge deck under skew winds - Part II: flutter derivatives", *J. Wind Eng. Ind. Aerodyn*, **90**, 807-837.

CC